

1 Beyond resource selection: emergent spatio-temporal 2 distributions from animal movements and stigmergent 3 interactions

4 Jonathan R. Potts^{1,a}, Valeria Giunta¹, Mark A. Lewis²

5 **1** School of Mathematics and Statistics, University of Sheffield, Hicks Building, Hounsfield Road, Sheffield, S3
6 7RH, UK

7 **2** Department of Mathematical and Statistical Sciences and Department of Biological Sciences, University of
8 Alberta, Edmonton T6G 2G1, Alberta, Canada

9 **a** Corresponding author. Email: j.potts@sheffield.ac.uk; Tel: +44(0)114-222-3729

10 **Abstract**

11 A principal concern of ecological research is to unveil the causes behind observed spatio-
12 temporal distributions of species. A key tactic is to correlate observed locations with en-
13 vironmental features, in the form of resource selection functions or other correlative species
14 distribution models. In reality, however, the distribution of any population both affects and
15 is affected by those surrounding it, creating a complex network of feedbacks causing emergent
16 spatio-temporal features that may not correlate with any particular aspect of the underlying
17 environment. Here, we study the way in which the movements of populations in response to one
18 another can affect the spatio-temporal distributions of ecosystems. We construct a stochastic
19 individual-based modelling (IBM) framework, based on stigmergent interactions (i.e. organisms
20 leave marks which cause others to alter their movements) between and within populations. We
21 show how to gain insight into this IBM via mathematical analysis of a partial differential equa-
22 tion (PDE) system given by a continuum limit. We show how the combination of stochastic
23 simulations of the IBM and mathematical analysis of PDEs can be used to categorise emer-
24 gent patterns into homogeneous vs. heterogeneous, stationary vs. perpetually-fluctuating, and

25 aggregation vs. segregation. In doing so, we develop techniques for understanding spatial
26 bifurcations in stochastic IBMs, grounded in mathematical analysis. Finally, we demonstrate
27 through a simple example how the interplay between environmental features and between-
28 population stigmergent interactions can give rise to predicted spatial distributions that are
29 quite different to those predicted purely by accounting for environmental covariates.

30 **Key words:** animal movement, animal space use, individual based models, partial differential
31 equations, resource selection, species distribution models, stigmergy

32 1 Introduction

33 Understanding the processes behind the spatial distributions of animal populations has been
34 a core concern of ecological research throughout its history (Elton, 2001; Nathan *et al.*, 2008).
35 Today, the need to manage the effects of rapid anthropogenic actions on ecosystems makes
36 predictive tools for spatial ecology more important than ever (Azaele *et al.*, 2015; Maris *et al.*,
37 2018). However, spatial ecology is complicated by the fact that the distribution of a population
38 of organisms will affect the distributions of those populations that surround it, and also be
39 affected by these populations (Morales *et al.*, 2010; Ovaskainen & Abrego, 2020). This generates
40 a complex network of feedbacks between the constituent populations of an ecosystem, causing
41 spatio-temporal patterns that can be difficult to predict, and impossible without the correct
42 mathematical and computational tools linking process to pattern (May, 2019; Potts & Lewis,
43 2019).

44 There are two principal processes by which space use can be affected by interactions between
45 populations (we use the word ‘population’ loosely, referring to anything ranging from a small
46 group such as a territorial unit or herd through to an entire species). First, interactions can
47 affect *demographics*, i.e. birth- and death-rates. This can be, for example, through predator-
48 prey interactions or competition for resources, both of which are well-known to have non-trivial
49 effects on both the overall demographic dynamics and the spatial distribution of species (Holmes
50 *et al.*, 1994; Tilman *et al.*, 1997; Okubo & Levin, 2001; Cantrell & Cosner, 2004; Lewis *et al.*,
51 2013, 2016).

52 Second, for mobile organisms, population interactions can affect the *movement* of individ-
53 uals (Mitchell & Lima, 2002; Vanak *et al.*, 2013; Breed *et al.*, 2017; Matthews *et al.*, 2020).
54 It is well-known, from the mathematical literature, that the two processes of demographics
55 and movement can combine to affect spatial distribution patterns in non-trivial ways, as ex-
56 emplified by studies of cross-diffusion and prey-taxis (Shigesada *et al.*, 1979; Lee *et al.*, 2009;
57 Gambino *et al.*, 2013; Potts & Petrovskii, 2017; Han & Dai, 2019; Haskell & Bell, 2020). These
58 studies typically model movement and demographics in the same system of equations (usually

59 partial differential equations), implying that the movements are occurring on the same spatio-
60 temporal scale as the demographics. Therefore the movements considered in such studies are
61 usually dispersal events. However, many animal populations can make significant movements
62 to rearrange themselves in space over timescales where births and deaths are negligible (Moor-
63 croft *et al.*, 2006; Vanak *et al.*, 2013; Ellison *et al.*, 2020). This particularly applies to larger
64 animals, such as birds, mammals, and reptiles, who have great capability for movement but
65 may only reproduce at a particular time of the year (e.g. spring). Therefore it is important
66 to understand how movement processes alone may affect spatio-temporal population patterns
67 (Potts & Lewis, 2019).

68 Spurred by rapid improvements in animal tagging technology, the empirical study of move-
69 ment has surged, with data being gathered at ever higher resolutions (Williams *et al.*, 2020).
70 Furthermore, an increasing number of studies are measuring animal interactions via the co-
71 tagging of multiple animals and new techniques for decoding the resulting information (Vanak
72 *et al.*, 2013; Potts *et al.*, 2014c; Schlägel *et al.*, 2019). A key goal of movement ecology is
73 to understand animal space use, so the question of how fine-grained movement and interac-
74 tion processes upscale to broader spatio-temporal patterns is gaining significant methodolog-
75 ical attention (Avgar *et al.*, 2016; Signer *et al.*, 2017; Potts & Schlägel, 2020). However, to
76 make predictions requires a theoretical understanding of how movements mediated by between-
77 population interactions affect space use. Our principal aim here is to provide the theoretical
78 framework for answering such questions.

79 To this end, we construct a general and extensible individual-based model (IBM) of move-
80 ments and interactions between multiple populations. We assume that animals, left alone on
81 the landscape, will have some sort of movement process allowing them to embark on daily
82 activities such as foraging. We model this very simply as a nearest-neighbour lattice random
83 walk (Okubo & Levin, 2001; Codling *et al.*, 2008). This is a foundational movement model,
84 which can be readily extended if one is interested in the finer details of foraging activity.

85 In this study, however, our focus is on the interactions between individuals and populations.

Mutual attraction:



Mutual avoidance:



Pursue-and-avoid:

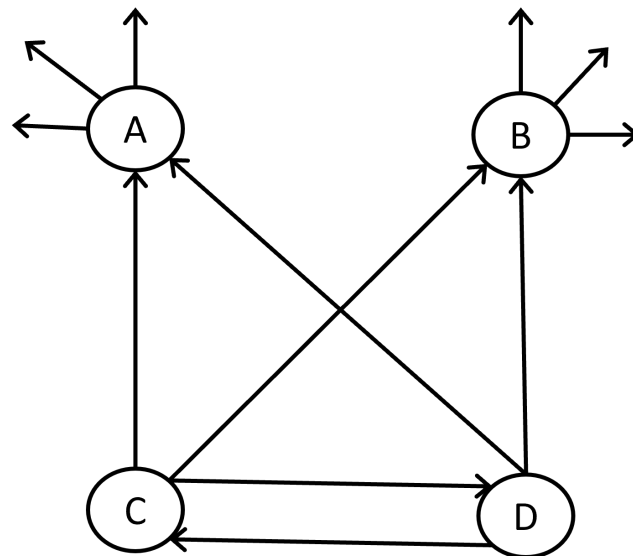
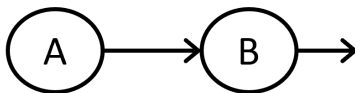


Fig. 1. Schematic diagram of stigmergent interactions. The left-hand side shows the three possible pairwise interactions between two populations. On the right is an example network built from these interactions. One might imagine that A and B are competing prey being predated by mutualistic predators C and D.

86 For this, we assume that, as individuals move, they leave a trace of where they have been on
87 the landscape, which could be in the form of scent, visual or olfactory marks, feces or a simply
88 a trail. These marks decay over time if the area is not revisited. Consequently, each population
89 leaves a distribution of such marks on the landscape, which changes over time as the constituent
90 individuals move about. Individuals of a population alter their movement according to the
91 presence or otherwise of marks, both from their own population and from others.

92 This process of leaving marks that cause others to alter their movement is called stigmergy,
93 and has been studied in various contexts, including collective animal movement and territorial
94 formation (Theraulaz & Bonabeau, 1999; Giuggioli *et al.*, 2013; White *et al.*, 2020). For any
95 given pair of populations, A and B, one could either have mutual avoidance (where individuals
96 from A avoid the marks of B and B avoid those of A), mutual attraction (individuals from
97 A and B are attracted to the marks of one another), or pursuit-and-avoidance (individuals
98 from A are attracted to marks of B but those from B avoid the marks of A). These combine

99 into a network of stigmergent interactions that together determine the overall spatio-temporal
100 distribution of the constituent populations (Figure 1). Our model is a generalisation of previous
101 models of territory formation from stigmergent interactions (Giuggioli *et al.*, 2011, 2013; Potts
102 *et al.*, 2012). However, these previous models were restricted to mutual avoidance processes
103 and typically had only one individual per ‘population’ (recall, we are using ‘population’ quite
104 generically here and could mean anything from a territorial unit to a larger group to a whole
105 species, depending on context).

106 As well as stochastic simulation analysis, we also examine the continuum limit of our IBM
107 model in space and time (i.e. as the lattice spacing and time step go to zero). We construct the
108 IBM so that this limit is a system of partial differential equations (PDEs) studied previously
109 in Potts & Lewis (2019). This formal connection between IBM and PDE enables us to use
110 the mathematical tools of PDE analysis to gain insight into the expected behaviour of the
111 IBM, which we can verify through simulation. The resulting techniques allow us to use PDE
112 analysis as a starting-point for exploring IBM models. This is valuable because PDEs are
113 amenable to mathematical analysis, enjoying a huge history of analytic techniques (Evans,
114 2010; Murray, 2012). However, IBMs are closer to reality and may be more amenable to
115 extensions that incorporate further realism beyond what is studied here (for example, realistic
116 movement processes based on life history needs such as foraging and tending to young). Such
117 formal connections between IBMs and PDEs are powerful as they enable the best of both
118 worlds: combining rigorous mathematical analysis with realistic modelling.

119 Finally, we explain how to account for landscape heterogeneity in our model, through
120 coupling our IBM to a step selection function (Fortin *et al.*, 2005; Potts *et al.*, 2014a; Avgar
121 *et al.*, 2016). We illustrate this with a simple example of two co-existing populations competing
122 for the same resource, inspired by wolf-coyote coexistence in the Greater Yellowstone Ecosystem
123 (Arjo & Pletscher, 2000). We investigate how the inclusion of interactions between and within
124 the populations combine with the heterogeneous landscape. We show how this combination
125 can cause emergent spatio-temporal patterns that cannot be explained merely by examining

126 the effect of landscape heterogeneity on animal space use (as is the norm in resource selection
127 studies and many other species distribution models).

128 A central theme that runs throughout this paper is that correlative models are not suf-
129 ficient for predicting space use patterns of multiple species in novel environments. This can
130 be illustrated by a simple thought experiment. Imagine there are two populations, each of
131 whose space use is affected by the other. One could understand the effect of population A on
132 the space use of population B by using a correlative model, such as resource or step selection,
133 with population B as the response variable and A as the explanatory variable. But then to
134 predict the space use of B in a novel environment, one would need to know *a priori* the space
135 use of A. Flipping this, one could put the distribution of A as the response variable and B as
136 explanatory. But then predicting the space use of A requires *a priori* knowledge about B. If
137 there is a novel environment where one does not know about the space use of either A or B then
138 correlative models (including joint species distribution models) cannot be used for prediction.
139 Instead a dynamic model is needed, such as an IBM or PDE. Although such IBMs and PDEs
140 can be *parametrised* by correlative techniques (Schlägel *et al.*, 2019; Potts & Schlägel, 2020),
141 *prediction* in a multi-population situation needs techniques beyond correlation. Our purpose
142 here is to make inroads into building these techniques.

143 Overall, our study aims to provide both insights into the effect of stigmergent interactions
144 between populations on the spatio-temporal distribution of mobile species, and provide extensi-
145 ble methods for studying these emergent features. This complements the burgeoning statistical
146 field of joint species distribution modelling, which gives tools for inferring the effect of one (or
147 more) species on the distribution of another (Ovaskainen & Abrego, 2020), whilst also enhanc-
148 ing this field by demonstrating the importance of considering the nonlinear feedbacks between
149 the movement processes of constituent populations for understanding spatial distributions.

150 2 Methods

151 2.1 The model

152 Our model of animal movement and stigmergent interactions is based on a nearest-neighbour
153 lattice random walk formalism. We work on an $L \times L$ square lattice, Λ . We choose periodic
154 boundary conditions for simplicity of presentation, although other forms are possible. We
155 assume that there are N populations and that, for each index $i = 1, \dots, N$, population i consists
156 of M_i individuals. Individuals leave marks at each lattice site they visit, and those marks decay
157 geometrically over time. For simplicity, one can think of these marks as scent, such as faeces
158 or urine, but they could correspond to any form by which animals may leave a trace of their
159 presence on the environment. The movement of each individual is biased by the presence of
160 marks from both their own population and others. For each population, this bias could be either
161 attractive or repulsive, depending on whether it is beneficial or detrimental for individuals
162 of one population to be in the presence of another population. Since animals look at their
163 surroundings at a distance to make movement decisions, our model allows for individuals to
164 respond to the local average density of nearby marks.

165 Mathematically this situation can be described by writing down the probability $f(\mathbf{x}, t +$
166 $\tau | \mathbf{x}', t)$ of moving from lattice site \mathbf{x}' to \mathbf{x} in a timestep of length τ . This function f is known
167 as a *movement kernel*. To construct our movement kernel, we use a generalised linear model
168 to describe the attraction to, or repulsion from, the local average density of nearby marks. A
169 second equation is then required to describe how marks are averaged over space. Finally, the
170 deposition and decay of marks over time is given by a third equation. We now give precise
171 functional forms of these three equations in turn.

172 Letting l be the lattice spacing and $m_i(\mathbf{x}, t)$ be the density of marks from population i at

173 location \mathbf{x} at time t , the movement kernel is given by

$$174 \quad f(\mathbf{x}, t + \tau | \mathbf{x}', t) = \begin{cases} K_{\mathbf{x}'} \exp \left[\sum_{j=1}^N a_{ij} \bar{m}_j^\delta(\mathbf{x}, t) \right], & \text{if } |\mathbf{x} - \mathbf{x}'| = l, \\ 0, & \text{otherwise.} \end{cases} \quad (1)$$

175

176 Here $K_{\mathbf{x}'} = \sum_{\mathbf{x}} f(\mathbf{x}, t + \tau | \mathbf{x}', t)$ is a normalising constant ensuring that $f(\mathbf{x}, t + \tau | \mathbf{x}', t)$ is a
177 well-defined probability distribution; if $a_{ij} > 0$ (resp. $a_{ij} < 0$) then $|a_{ij}|$ is the strength of
178 population i 's attraction to (resp. repulsion from) population j ; and $\bar{m}_j^\delta(\mathbf{x}, t)$ represents the
179 average mark density over a radius of δ . Note that Equation (1) fits into the broad category of
180 functions that can be parametrised by integrated step selection analysis (Avgar *et al.*, 2016).

181 The equation for average mark density is

$$182 \quad \bar{m}_j^\delta(\mathbf{x}, t) = \frac{1}{|S_\delta|} \sum_{\mathbf{z} \in S_\delta} m_j(\mathbf{x} + \mathbf{z}, t), \quad (2)$$

183

184 where $S_\delta = \{\mathbf{z} \in \Lambda : |\mathbf{z}| < \delta\}$ is the set of lattice sites that are within a distance of δ from
185 0 and $|S_\delta|$ is the number of lattice sites in S_δ . Note that Equation (2) requires us to use
186 periodic boundary conditions, so that there are always the same number of lattice sites within
187 a distance of δ from any point in Λ . However, if we were to use hard boundaries, e.g. for
188 modelling movement near a coastline, we would have to take the average in Equation (2) over
189 the set $\{\mathbf{x} + \mathbf{z} \in \Lambda | \mathbf{z} \in S_\delta\}$.

190 The equation defining the change in marks over time, which are deposited by individuals
191 and then decay geometrically, is

$$192 \quad m_i(\mathbf{x}, t + \tau) = (1 - \mu_\tau) m_i(\mathbf{x}, t) + \rho_\tau \mathcal{N}_i(\mathbf{x}, t), \quad (3)$$

193

194 where $\mathcal{N}_i(\mathbf{x}, t)$ is the number of individuals at location \mathbf{x} in population i at time t , μ_τ is the
195 amount by which marks decay in a time step of length τ , and ρ_τ is the amount of marking
196 made by a single animal in a single time step.

197 Equations (1-3) are not the only available functional forms to describe our stigmergent
198 process. However, the specific form for Equation (1) is advantageous because it arrives in
199 the form of a step selection function (Fortin *et al.*, 2005; Avgar *et al.*, 2016). It thus has the
200 potential to be parametrised by the methods of Schlägel *et al.* (2019), which deals with step
201 selection for interacting individuals (although here we focus on analysing the emergent features
202 of the model in Equation (3) rather than the question of fitting this model to data.) Equation
203 (2) assumes that marks are averaged over a fixed disc around the individual and was chosen
204 for simplicity, but other options, such as exponentially decaying averaging kernels, are also
205 possible. Equation (3) was, likewise, chosen for simplicity.

206 One drawback is that there is, in theory, no limit on the amount of marks in one location. If
207 it is necessary to account for such a limit, one might exchange the $\rho_{\tau}\mathcal{N}_i(\mathbf{x}, t)$ term for something
208 like $\rho_{\tau}(1 - \mathcal{N}_i(\mathbf{x}, t)/\mathcal{N}_{\max})\mathcal{N}_i(\mathbf{x}, t)$, where \mathcal{N}_{\max} is the maximum number of marks at a single
209 location. However, we do not explore this extension in detail here; much insight can be gained
210 without needing to incorporate this extra complexity. Alternatively, one could replace ‘amount
211 of marks’ with ‘probability of mark presence’. Since probabilities are bounded between 0 and
212 1, this would lead to a similar formalism as the situation where the number of marks has a
213 limit. Such a situation was studied in Potts & Lewis (2016) but is not considered here.

214 Finally, there is an analogy between marks and resource depletion that enables our mod-
215 elling framework to be used in situations where animals both deplete resources and move up
216 resource gradients. The idea is to view the total number of marks in a location, from all the
217 populations, as the extent of depletion of a resource. In this case, each population would avoid
218 ‘marks’ left by either population, as animals will tend to avoid depleted resources. We do
219 not explicitly examine this situation here, but it is a possibility for future investigations and
220 expands the potential applicability of our work.

221 2.2 Methods for analysing simulation output

222 We analyse the individual-based model (IBM) from Equations (1-3) using stochastic simula-
223 tions. Example simulation runs reveal a range of patterns (Fig. 2). Here, we detail methods
224 for characterising these via three broad questions: (I) Is the distribution of animal locations
225 heterogeneous or homogeneous? (II) If heterogeneous, do the patterns stabilise over time, so
226 that populations keep broadly to fixed areas of space, or do they undergo persistent fluctua-
227 tions? (III) For any two populations, are they segregated from one another or aggregated in
228 the same small area? The stochastic nature of the IBM means that there will always be some
229 amount of heterogeneity and persistent fluctuations due to noise. Our methods thus need to
230 distinguish between what is noise and what is an actual pattern.

231 To answer question (I), we examine the local population density, $l_{i,d}(\mathbf{x}, t)$, averaged around
232 a disc of radius d , at each lattice site x and time t , for each population i . At each point in
233 time, we compute the *amplitude* of the pattern as $A_{i,d}(t) = \max_{\mathbf{x}}[l_{i,d}(\mathbf{x}, t)] - \min_{\mathbf{x}}[l_{i,d}(\mathbf{x}, t)]$,
234 the maximum local population density across space minus the minimum. We want to find out
235 whether the amplitude ever becomes higher than would be expected from individuals moving
236 as independent random walkers (i.e. when $a_{ij} = 0$ for all i, j in Equation 1), assuming that the
237 individuals are initially distributed uniformly at random on the lattice. For this, we calculate
238 $A_{i,d}(t)$ in the case $a_{ij} = 0$ for all i, j (i.e. no mark deposition so no interactions between walkers)
239 and take the average over a sufficiently long time period to calculate the mean to a given degree
240 of accuracy (i.e. so that the standard deviation of the mean is below a pre-defined threshold,
241 determined by the needs of the simulation experiment). We call this mean amplitude A_{rw} (for
242 ‘random walk’). Then the extent to which the patterns are heterogenous can be determined
243 with reference to this base-line value.

244 Question (II) requires that we keep track of the mean location of individuals in each popu-
245 lation. Since individuals are moving on a lattice with periodic boundary conditions, it is
246 necessary to take a circular mean (Berens, 2009). However, if individuals are roughly uni-
247 formly spread in either the horizontal or vertical direction then the circular mean can be very

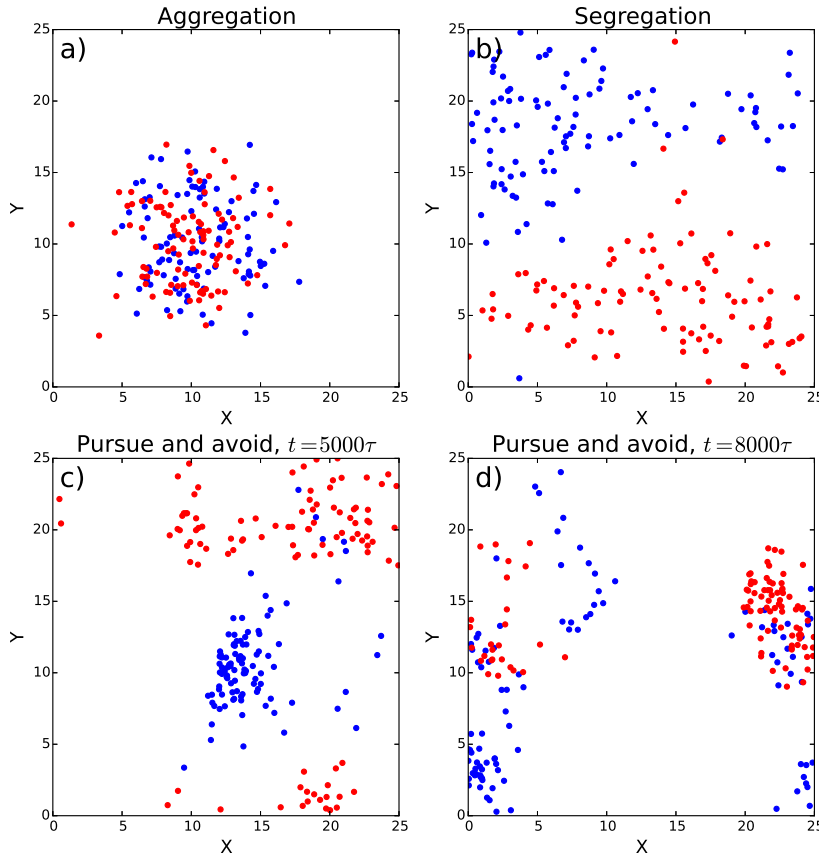


Fig. 2. Example snapshots of simulation output. In all panels, two populations of 100 individuals each were simulated on a 25×25 lattice, with initial locations distributed uniformly at random on the landscape. Also $\mu = 0.001$ and $\rho = 0.01$ for all panels (Equation 3). Panel (a) shows a system where two populations form a single, stable aggregation. Here, $a_{11} = a_{22} = 0$, $a_{12} = a_{21} = 2$, $\delta = 10l$ (Equation 1). In panel (b) the populations segregate into distinct parts of space. Here, $a_{11} = a_{22} = 0$, $a_{12} = a_{21} = -2$, and $\delta = 5l$. In both Panels (a) and (b) the snapshot is taken at time $t = 5000\tau$. Panels (c) and (d) show a situation where one population (blue) chases other (red) around the landscape in perpetuity, with snapshots at two different times. Here, $a_{11} = a_{22} = 1$, $a_{12} = 10$, $a_{21} = -10$, and $\delta = 10l$.

248 sensitive to stochastic fluctuations. We therefore introduce a *corrected circular mean* which
 249 accounts for this, and denote it by $\mathbf{c}_i(t)$ (notice that this is a location in two dimensions, for
 250 each time, t). Precise details of how to calculate $\mathbf{c}_i(t)$ are given in Supplementary Appendix

251 A.

252 As with the amplitude calculations, we need to determine whether changes in $\mathbf{c}_i(t)$ are
253 indicative of a fluctuating pattern (like in Figs. 2c,d) or just noise around an essentially
254 stationary population distribution (as in Figs. 2a,b). For any length R and time-interval, T ,
255 we say that a system has become (R, T) -stable at time T_* if $|\mathbf{c}_i(T_* + t) - \mathbf{c}_i(T_*)| < R$ for each
256 population i whenever $0 \leq t \leq T$. For example, the systems in Figs. 2a,b are both $(l, 1000\tau)$ -
257 stable, but the system shown in Figs. 2c,d is not. In Section 2.3 we will show how to choose
258 values of R and T , by ensuring they are consistent with the results of mathematical analysis.

259 For Question (III), the extent to which a pair of populations i, j ($i \neq j$) is aggregated or
260 segregated at any point in time is measured using the *separation index*, $s_{ij}(t) = |\mathbf{c}_i(t) - \mathbf{c}_j(t)|$.
261 For systems that become (R, T) -stable at some time T_* , we can define the asymptotic separation
262 index s_{ij}^* as the average of $s_{ij}(t)$ across $T_* < t < T_* + T$. A separation index close to 0 indicates
263 that the populations are occupying a similar part of space. If we know, from Question (I), that
264 both populations are displaying heterogeneous patterns then in this case we have an aggregation
265 of both populations. Higher separation indices, coupled with the existence of heterogeneous
266 patterns, are suggestive of segregation patterns.

267 The separation index is a simple metric that is quick to calculate for multiple simulation
268 analysis. However, one could also use more sophisticated measures of range overlap, such as
269 the Bhattacharyya's Affinity (Fieberg & Kochanny, 2005) between kernel density estimators
270 (Worton, 1989; Fleming *et al.*, 2015). Here, though, we will keep things simple, to enable
271 analysis of a broader range of simulation scenarios in a realistic time-frame.

272 **2.3 Mathematical techniques**

273 Techniques for analysing the output of stochastic IBMs can involve choices that might be
274 somewhat arbitrary, for example the choices of T_{amp} , R , and T in Section 2.2. Therefore it
275 is valuable to ground-truth these choices by means of mathematical analysis. In particular,
276 we do this via a PDE approximation describing the probability distribution of individuals for

277 each population. In PDE theory, patterns can emerge when a change in parameter causes
 278 the system to switch from a situation whereby the constant steady state (corresponding to
 279 homogeneously distributed individuals) becomes unstable, leading to the distribution tending
 280 to either a non-constant steady state (heterogeneously distributed individuals), or entering a
 281 perpetually fluctuating situation. The parameter value where the switch occurs is called a
 282 bifurcation point. The nature of this bifurcation point can be ascertained by a combination
 283 of linear stability analysis (LSA) and weakly non-linear analysis. Here we focus on LSA for
 284 simplicity (which is also called Turing pattern analysis, after Turing (1952)).

285 To arrive at a PDE system, we take a continuous limit in both space and time, sending
 286 l and τ to 0 such that l^2/τ tends to a finite constant, $D > 0$. This is sometimes called the
 287 diffusion limit, as D is a diffusion constant, but is also referred to as the parabolic limit (Hillen
 288 & Painter, 2013). If we take this limit, and also assume that infinitesimal moments beyond the
 289 second are negligible, we arrive at the following system of PDEs (see Supplementary Appendix
 290 B for details)

$$291 \quad \frac{\partial u_i}{\partial t} = \underbrace{D\nabla^2 u_i}_{\text{Diffusive movement}} - \underbrace{2D\nabla \cdot \left[u_i \nabla \sum_{j=1}^N a_{ij} \bar{q}_j^\delta \right]}_{\text{Advection due to presence of marks}}, \quad (4)$$

$$292 \quad \frac{\partial q_i}{\partial t} = \underbrace{\rho u_i}_{\text{Mark deposition}} - \underbrace{\mu q_i}_{\text{Mark decay}}, \quad (5)$$

293

294 for each $i = 1, \dots, N$, where $u_i(\mathbf{x}, t)$ is the location density of population i , $q_i(\mathbf{x}, t)$ is the density
 295 of marks, ρ is the limit of $\frac{\rho_\tau}{\tau}$ as $\rho_\tau, \tau \rightarrow 0$, μ is the limit of $\frac{\mu_\tau}{\tau}$ as $\mu_\tau, \tau \rightarrow 0$, and $\bar{q}_j^\delta(\mathbf{x}, t)$ is
 296 the average of $q(\mathbf{x}, t)$ over a ball of radius δ . Here, we assume that animals move at the same
 297 rate, so D is independent of i . It is possible to drop this assumption, and we discuss the effect
 298 of doing this in Supplementary Appendix C. However, for simplicity of calculations we keep D
 299 constant in the Main Text.

300 It is sometimes helpful to simplify calculations by assuming that q_i equilibrates much faster
 301 than u_i , so that the scent mark is in quasi-equilibrium ($\frac{\partial q_i}{\partial t} = 0$), leading to the following

302 equation for each $i = 1, \dots, N$

$$303 \quad \frac{\partial u_i}{\partial t} = D \nabla^2 u_i - \frac{2D\rho}{\mu} \nabla \cdot \left[u_i \nabla \sum_{j=1}^N a_{ij} \vec{q}_j^\delta \right]. \quad (6)$$

304

305 This assumption says, in effect, that the distribution of marks accurately reflects the space
306 use distribution of the population. When terrain marking is deliberate, its usual purpose is
307 precisely to advertise space use. Therefore this quasi-equilibrium assumption is likely to be
308 biologically reasonable in many realistic situations.

309 The LSA technique enables us to use Equations (4-5) to construct the *pattern formation*
310 *matrix*, \mathcal{M} (see Supplementary Appendix C for the full expression and derivation). The eigen-
311 values of \mathcal{M} give key information about whether heterogeneous patterns will spontaneously
312 form from small perturbations of a homogeneous system (i.e. individuals initially uniformly
313 distributed on the landscape), and also whether these patterns begin to oscillate as they emerge.
314 This technique dates back to Turing (1952) and is essentially an extension to PDEs of stability
315 analysis for ordinary differential equations (May, 2019).

316 The emergence of heterogeneous patterns is expected whenever there is an eigenvalue whose
317 real part is positive. Thus the sign of the eigenvalue with biggest real part (a.k.a. the dominant
318 eigenvalue) gives an indication of the answer to Question (I) above. If the dominant eigenvalue
319 has positive real part and a non-zero imaginary part then small perturbations of the homoge-
320 neous system will oscillate as they grow, at least at small times. Often (but not always) these
321 oscillations will persist for all times, so give an indication of the likely answer to Question (II).
322 We stress that this is just an indication, though, and that discrepancies may exist between the
323 answer to (II) and whether or not the dominant eigenvalue of \mathcal{M} is real. Full analysis of when
324 to expect non-constant stationary patterns in Equation (4-5), or when to expect perpetually
325 changing patterns, requires more sophisticated techniques.

326 2.4 Simulation experiments

327 To give some insight into the sort of patterns that can emerge from our model (Equations 1-3),
328 we perform a variety of simulations in the simple case of two populations ($N = 2$). Throughout,
329 we assume that each population has 100 individuals ($M_1 = M_2 = 100$) and we work on a 25×25
330 lattice. We assume $\tau = 1$ and $l = 1$ so can write $\mu_\tau = \mu$ and $\rho_\tau = \rho$ for ease of notation. We
331 also assume $\delta = 5$ throughout.

332 First, we examine the situation where populations have a symmetric response to one an-
333 other, so that $a_{12} = a_{21} = a$. For simplicity, we set $a_{11} = a_{22} = 0$. In this case the continuum
334 limit PDE system (Equations 4-5) has the following pattern formation matrix (derived in Sup-
335 plementary Appendix C)

$$336 \quad \mathcal{M} = \begin{pmatrix} -\kappa^2 & 0 & 0 & \frac{8a}{25}\kappa^2 \\ 0 & -\kappa^2 & \frac{8a}{25}\kappa^2 & 0 \\ \rho & 0 & -\mu & 0 \\ 0 & \rho & 0 & -\mu \end{pmatrix}. \quad (7)$$

337

338 Here, κ is the wavenumber of the patterns that may emerge at small times, if there is an
339 eigenvalue of \mathcal{M} with positive real part (i.e. the wavelength of these patterns would be $2\pi/\kappa$).
340 For our simulation experiments, we fix the scent-marking rate $\rho = 0.01$ to be a low number and
341 vary the decay rate μ . We consider two different values of a : either $a = 2$, which corresponds
342 to populations having a mutual attraction, or $a = -2$, corresponding to mutual avoidance.
343 In either case, the dominant eigenvalue of \mathcal{M} is always real (Supplementary Appendix C).
344 Furthermore, it is positive if and only if $\mu < 0.0064$. In other words, this mathematical
345 analysis predicts that the system will bifurcate at $\mu = 0.0064$ from homogeneous patterns
346 ($\mu > 0.0064$) to heterogeneous patterns ($\mu < 0.0064$). This means that if marks remain long
347 enough on the landscape, they will affect movement to such an extent that the overall space
348 use patterns change from being homogeneous (so indistinguishable from independent random
349 walkers) to heterogeneous. This heterogeneity will be either aggregative, if $a = 2$, analogous

350 to the example in Figure 2a or segregative, if $a = -2$, like Figure 2b.

351 To test whether we see a similar change in stability in simulations, we start by simulating
352 our system in the case $\mu = 0.009$, run this until it is (R, T) -stable for $R = 1$ and $T = 1000$
353 and measure the asymptotic amplitude, $A_{i,d}^*$ for $i = 1, 2$, by averaging $A_{i,d}(t)$ over the 10000
354 time steps after (R, T) -stability has been achieved. For this, we use $d = 5$. We then use
355 the final locations of each individual as initial conditions in our next simulation run, which is
356 identical except for choosing $\mu = 0.0069$. We iterate this process, reducing μ by 0.0001 each
357 time, until $\mu = 0.001$. This mimics the numerical bifurcation analysis often performed when
358 analysing PDEs (Painter & Hillen, 2011). We perform this whole iterative process for both
359 $a = 2$ and $a = -2$, the expectation being that $A_{i,d}^*$ will be approximately the same as that of
360 non-interacting individuals (A_{rw}) until the value of μ crosses $\mu = 0.0064$, at which point we
361 expect $A_{i,d}^*$ to start increasing.

362 To investigate whether linear stability analysis of the PDE system (Equations 4-5) reflects
363 our method for answering Question (II), we set $a_{11} = a_{22} = 1$, $\rho = 0.01$, $\mu = 0.002$, and
364 sample a_{12} and a_{21} uniformly at random, 100 times each, from the interval $[-5, 5]$. To make
365 calculations more transparent, we assume that the scent marks are in quasi-equilibrium, taking
366 the adiabatic approximation in Equation (6). In this case the pattern formation matrix is

$$367 \quad \mathcal{M} = \frac{1}{5} \begin{pmatrix} 3 & 8a_{12} \\ 8a_{21} & 3 \end{pmatrix}, \quad (8)$$

368

369 and so the dominant eigenvalue is $(15 + 4\sqrt{a_{12}a_{21}})/25$. If the cross interaction terms are of
370 identical sign ($a_{12}a_{21} > 0$) then linear stability analysis predicts stationary patterns to emerge
371 (at least at small times), but if they are of different sign ($a_{12}a_{21} < 0$) then the dominant
372 eigenvalue is not real, so patterns should oscillate as they emerge. The latter case corresponds
373 to the type of pursuit-and-avoidance situation that we see in Fig. 2c,d. We compare these
374 predictions to our definition of (R, T) -stability for a range of values of R and T to ascertain
375 the extent to which the separation between real and non-real eigenvalues corresponds to the

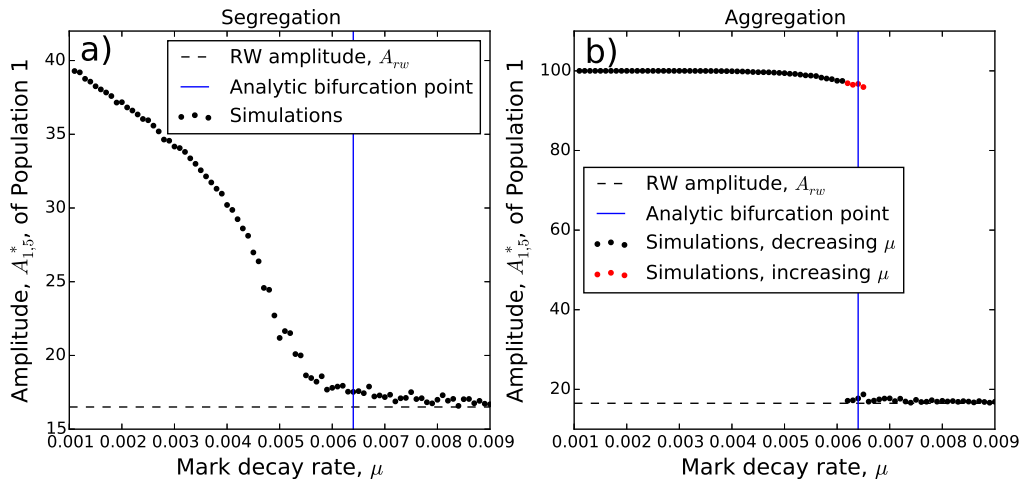


Fig. 3. Pattern formation analysis of stochastic simulations for $N = 2$. Each panel shows, using solid dots, the amplitude, $A_{1,5}^*$, of Population 1 for different values of μ , where $\rho = 0.01$, $a_{12} = a_{21} = a$, and $a_{11} = a_{22} = 0$. Black dots represent the situation where μ is decreased progressively (see Section 2.4 for details) and red dots show the situation where μ is increased (Section 3). In Panel (a), $a = -2$ so that the populations repel one another and in Panel (b), $a = 2$ so populations are attractive. The value A_{rw} , the amplitude in the situation where each individual is a non-interacting random walker, is given by the dashed black line. The blue line gives the bifurcation point predicted by analysis of the continuum limit PDE, Equations (4)-(5), which gives an indication of where we expect the amplitudes of the simulations to become notably larger A_{rw} .

376 existence or not of (R, T) -stability.

377 2.5 Incorporating environmental effects

378 As mentioned at the end of Section 2.1, Equation (1) is in the form of a step selection function.
 379 This means that it can be readily used to incorporate the effect on movement of environ-
 380 mental or landscape features. Suppose that we have n such features, denoted by functions
 381 $Z_1(\mathbf{x}), \dots, Z_n(\mathbf{x})$. For each $k = 1, \dots, n$, denote by β_k the relative effect of $Z_k(\mathbf{x})$ on move-
 382 ment. Then, to incorporate these into the movement kernel, we modify Equation (1) as follows

$$383 \quad f(\mathbf{x}, t + \tau | \mathbf{x}', t) = \begin{cases} K_{\mathbf{x}'} \exp \left[\sum_{j=1}^N a_{ij} \bar{m}_j^\delta(\mathbf{x}, t) + \sum_{k=1}^n \beta_k Z_k(\mathbf{x}) \right], & \text{if } |\mathbf{x} - \mathbf{x}'| = l, \\ 0, & \text{otherwise.} \end{cases} \quad (9)$$

384

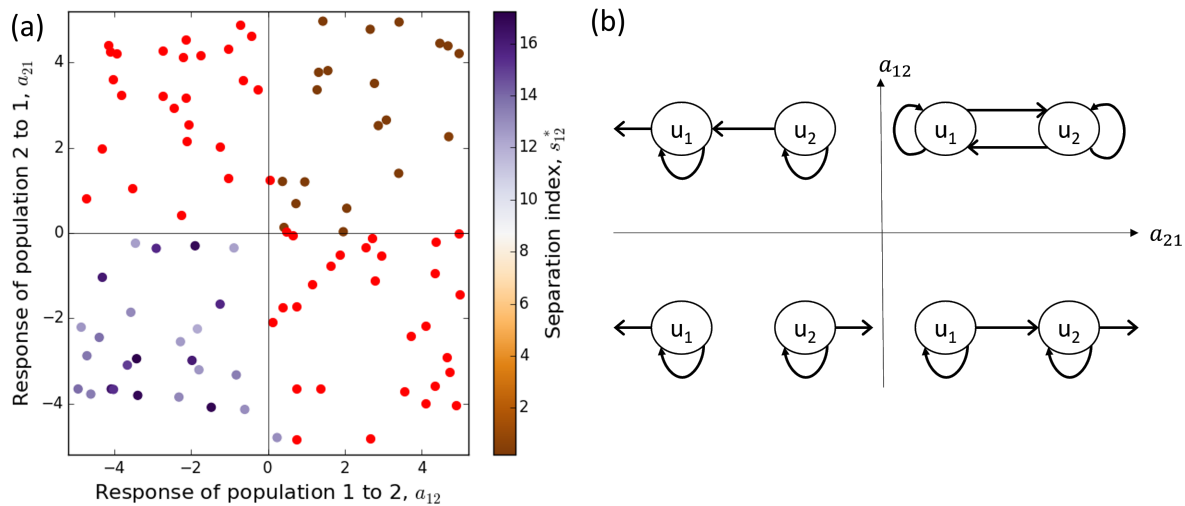


Fig. 4. Stability of emergent patterns. In Panel (a), each dot represents a simulation run of the IBM in Equations (1)-(3) where $a_{11} = a_{22} = 1$, $\rho = 0.01$, $\mu = 0.002$ and the values of a_{12} and a_{21} are given by the horizontal and vertical axes respectively. Red dots denote simulation runs that were not (R, T) -stable (for $R/l = 1$, $T/\tau = 7500$), whereas those on the purple-to-brown spectrum were (R, T) -stable. This colour spectrum corresponds to the separation index, from aggregative to segregative. Linear pattern formation analysis of the PDEs in Equations (4)-(5) predicts stationary (resp. non-stationary) patterns to emerge in the top-right and bottom-left (resp. top-left and bottom-right) quadrants, which corresponds well with the dot colours. Notice that the top-right (resp. bottom-left) quadrant corresponds to mutual attraction (resp. avoidance) and, likewise, the dot colours indicate aggregation (resp. segregation) patterns. Panel (b) gives a schematic of the between-population movement responses corresponding to the four quadrants in panel (a). An arrow from u_i to u_j represents attraction of population i towards population j . An arrow pointing out of u_i away from u_j represents u_i avoiding u_j .

385 We use this to investigate the effect on space use of interactions both between populations
 386 and with the environment, by considering a simple toy scenario, but one that is based on a
 387 particular empirical situation. Specifically, we consider two populations competing for the same
 388 heterogeneously-distributed resource, $Z_1(\mathbf{x})$ (here, $n = 1$). One population is assumed to be
 389 a weaker competitor, so avoids the stronger competitor, whilst the movements of the stronger
 390 are not affected by the weaker. Both have a tendency to move towards areas of higher-density
 391 resources.

392 In our simulations, each population consists of 100 individuals. We examine three cases.

R/l	T/τ	Agreement	SU/AS	SS/AU
0.5	5000	54%	46%	0%
1	5000	87%	0%	13%
1	7000	96%	0%	4%
1	7500	97%	2%	1%
1	8000	95%	5%	0%
2	5000	84%	0%	14%
2	7000	93%	0%	7%
2	7500	95%	0%	5%
2	8000	96%	4%	0%

Table 1. Extent to which analytic predictions agree with our simulation analysis for different choices of R and T . The third column gives the percentage of the simulations from Fig. 4 for which the analytic prediction for stability agrees with that measured from stochastic simulations using our method. The fourth (resp. fifth) gives the percentage for which the stochastic simulations were deemed unstable (resp. stable), for the given values of R and T , but the analytic prediction is stable (resp. unstable), denoted as SU/AS (rep. SS/AU).

393 The first is where the effect of the stronger competitor on the weaker is ignored (so animals
394 are assumed to act independently, which mirrors many basic resource/step selection studies).
395 The second incorporates the effect of the stronger on the weaker’s movements, but treats each
396 individual within a population as independent from the others in the population. This mirrors
397 some recent resource selection studies whereby the movement of one population is affected by
398 the presence of another, e.g. Vanak *et al.* (2013); Latombe *et al.* (2014). The third assumes
399 that the stronger population are highly territorial, so are split into five separate sub-groups,
400 each of which exhibit strong intra-group attraction but inter-group repulsion. The simulated
401 resource layer is a Gaussian random field on a 25×25 lattice, previously used in the context
402 of resource selection by (Potts *et al.*, 2014b). Precise details of the simulation experiments we
403 performed are given in Supplementary Appendix D.

404 Whilst this situation is a deliberately general and simplified model, it is inspired by the
405 particular situation of wolf-coyote coexistence in the Greater Yellowstone Ecosystem. Here, the
406 stronger competitor is the wolf population, coyotes being weaker, and the resource layer is the
407 distribution of where prey are likely to be found. The ability for coyotes to coexist with wolves
408 in this system has been conjectured to emerge from the territorial structures of wolves, which

409 include relatively large interstitial regions that may be havens for coyote (Arjo & Pletscher,
410 2000). If true, this means that the intra-pack attraction and inter-pack avoidance mechanisms
411 are key to understanding the space use of wolves and coyotes. The three models presented
412 here can be viewed as testing how the different assumptions about wolf-coyote and wolf-wolf
413 interactions might interface with resource selection to affect their space use distributions.

414 3 Results

415 Fig. 3 shows the results of pattern formation analysis of our IBM. The place at which the
416 amplitude grows higher than that of random non-interacting individuals is reasonably close to
417 the bifurcation point predicted by linear stability analysis of the corresponding continuum PDE
418 system. However, the latter occurs at a slightly lower value of μ than for the IBM indicating
419 that a slightly lower decay rate of marks is necessary to overcome the stochastic effects and
420 allow patterns to form. In other words, the stochasticity has a mild homogenising effect.

421 For negative a (recall $a = a_{12} = a_{21}$ in Equation 1), where we tend to see segregation
422 patterns beyond the bifurcation point, the amplitudes $A_{1,5}^*$, represented by black dots, appear
423 to grow steadily as μ is decreased (Fig. 3a). However, for positive a , there is a sudden jump
424 in the amplitude between $\mu = 0.0062$ and $\mu = 0.0061$ (Fig. 3b). Such jumps in bifurcation
425 diagrams can sometimes be accompanied by a hysteresis effect, whereby if the initial conditions
426 contain patterns then the patterns may persist even in parameter regimes where they would
427 not emerge spontaneously. To test this, we performed the same IBM pattern formation analysis
428 as before, but this time starting with $\mu = 0.0004$ and increasing μ by 0.0001 each iteration
429 (rather than decreasing as before). The red dots in Fig. 3b show that there is indeed hysteresis
430 in the IBM system, whereby the system is bistable for $0.006 \lesssim \mu \lesssim 0.0065$, a phenomenon
431 that has also been observed in single population aggregation models with a slightly different
432 class of differential equation models (Potts & Painter, 2021). This means that if a population
433 is already aggregated then μ would need to drop below about 0.006 for the aggregation to
434 collapse. Yet if a population is not already aggregated, μ would have to increase above 0.0065

435 for aggregations to form.

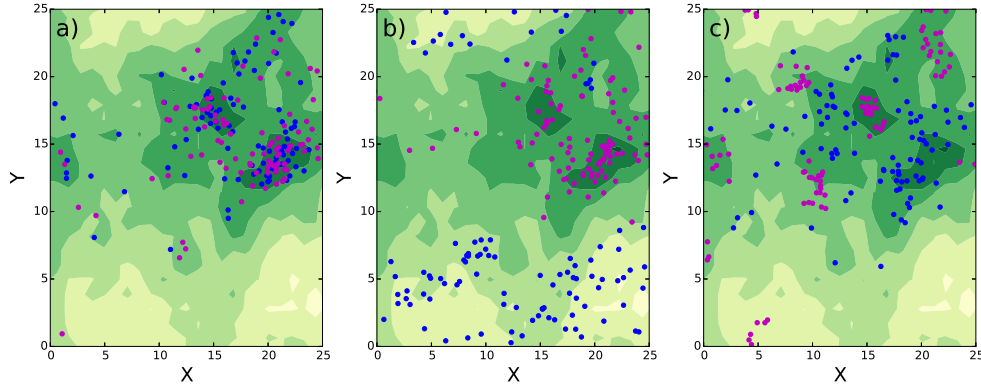


Fig. 5. Incorporating environmental effects. This figure shows the space use distributions that emerge from three different scenarios involving two populations attracted to the same heterogeneously-distributed resource. This resource is shown in shades of yellow-green, with darker (resp. lighter) green denoting higher (resp. lower) density of resources. Magenta (resp. blue) dots denote the stronger (resp. weaker) competitor. In Panel (a) the individuals do not alter their movement in response to the presence of others, and we simply see a preference for higher quality resources. In Panel (b), as well as attraction to better resources, the weaker (blue) population has a tendency to move away from the stronger (magenta) population. In addition to this avoidance mechanism, in Panel (c) the magenta population is strongly territorial. This leads to the emergence of interstitial regions where the blue population can access resources that may be quite high quality.

436 Fig. 4 shows that (R, T) -stability corresponds well to the predictions of pattern formation
437 analysis in the case where $R = l$ and $T = 5000\tau$. These were the best values of R and T
438 we found from the ones tested, inasmuch as the results corresponded to the pattern formation
439 analysis in the highest proportion of cases, $N\%$ (Table 1). Notice too that the mutually-
440 avoiding populations (with $a_{12}, a_{21} < 0$) tend to have much higher separation indices, s_{12}^* , than
441 the mutually attracting populations, as one would expect.

442 Fig. 5 shows the results of our three simulation experiments on a heterogeneous resource
443 landscape. When we assume that there are no inter-population interactions then the result-
444 ing model predicts space-use patterns whereby both populations have very similar space use
445 distributions (Fig. 5a). When we account for the avoidance of the weaker population by the
446 stronger then the model predicts that the stronger population will live where the resources are

447 better, driving the weaker to resource-poor areas (Fig. 5b). This, of course, may ultimately
448 lead to the weaker population being unable to survive. However, if the stronger population is
449 strongly territorial, it can subdivide into separate groups, leaving interstitial regions where the
450 weaker population can survive and have access to resources that may be relatively high quality
451 (Fig. 5c).

452 4 Discussion

453 Resource selection analysis is one of the most popular techniques for understanding the distri-
454 bution of species and populations. However, like many species distribution models, studies tend
455 to focus on correlating animal locations with environmental and landscape features. Whilst
456 some more recent studies in resource selection (Bastille-Rousseau *et al.*, 2015), step selection
457 (Vanak *et al.*, 2013), and species distribution modelling (Ovaskainen & Abrego, 2020) have
458 examined the way presence of one population may affect that of another, the first population
459 tends to be treated as a static layer, similar to a resource layer, which then affects the presence
460 or movement of the second population. This assumption neglects the dynamic feedbacks that
461 can occur between two or more populations of animals.

462 Here, we have shown that such feedbacks can generate a variety of emergent patterns that
463 can be quite different to those that appear when only accounting for static layers (Fig. 5).
464 We have given a basic categorisation scheme for these patterns via simple binary questions:
465 homogeneous or heterogeneous, stable or dynamic, segregated or aggregated. We have shown
466 that, even with just two populations, all these patterns are possible. This categorisation,
467 however, is likely to be only the tip of the iceberg in terms of the possible patterning properties
468 arising from sigmoid interactions between multiple populations. Indeed, a recent study
469 of the limiting deterministic PDE (Potts & Lewis, 2019) unveiled a rich suite of patterns
470 through numerical simulations, including all those patterns studied here, as well as period
471 doubling bifurcations, travelling-waves, and irregular patterns suggestive of chaos. Although
472 such subtleties in pattern formation may be tricky to distinguish from noise in an IBM, it is

473 valuable to be aware that they may yet be present in real systems.

474 Whilst a coarse-grained, individual-based approach to ecological modelling is valuable in
475 ensuring emergent phenomena are not simply an outcome of continuum assumptions (Durrett
476 & Levin, 1994; Getz *et al.*, 2018), here our limiting PDE has been very valuable for gaining
477 insight into our IBM. First, understanding the places where the PDE system bifurcates from
478 between different patterning regimes has enabled us to identify interesting parameter regimes
479 for studying our IBM (Figs. 3 and 4). Second, comparison between patterns in our IBM
480 and the corresponding PDE has enabled us to tune the various otherwise-arbitrary choices
481 of parameters used in analysing IBMs (e.g. the choices of R and T determined by Table 1).
482 Whilst there is a tradition of ecological studies where limiting PDEs have helped decode the
483 complexity inherent in IBMs (Durrett & Levin, 1994; Sherratt *et al.*, 1997; Hosseini, 2006), this
484 is perhaps overshadowed by the recent prevalence of IBM-only studies in ecology (Grimm, 1999;
485 Grimm & Railsback, 2013; DeAngelis, 2018). We hope our use of PDEs here helps encourage
486 further studies to implement PDEs as a tool for understanding IBMs.

487 Here, we have explored pattern formation analysis of PDEs using perhaps the simplest
488 tool, that of linear analysis. However, there are plenty of other tools, with varying conceptual
489 and mathematical complexity, that may provide insight. For example, in Fig. 3a, we see that
490 patterns emerge smoothly as one decreases μ past the bifurcation point, which is suggestive
491 of a super-critical bifurcation. However, in Fig. 3b, there is a sudden jump, together with
492 a hysteresis (bistable) region, something usually accompanied by a sub-critical bifurcation.
493 Techniques such as weakly non-linear analysis (Eftimie *et al.*, 2009) and Crandall-Rabinowitz
494 abstract bifurcation theory (Buttenschön & Buttenschön, 2021) are able to distinguish rigor-
495 ously between these two cases. These are, however, much more conceptually and technically
496 demanding than linear analysis, and will require a significant, separate work.

497 Even without advanced techniques for studying PDEs, though, we have shown how re-
498 searchers can gain insight through stochastic IBM experiments. To do this, we have developed
499 tools that mimic those used for understanding PDEs, but tailored for use with stochastic IBMs.

500 A principal technical obstacle was to separate-out random noise from actual spatial patterns,
501 be they stationary or fluctuating. The fact that our techniques agreed well with the analogous
502 PDE analysis provides a validation and ground-truthing of the methods, suggesting they are
503 capturing the key features of patterning with good accuracy.

504 Furthermore, even in the relatively simple example situations studied here, our IBM anal-
505 ysis revealed some interesting theoretical insights. It appears that segregation patterns emerge
506 in a continuous fashion as a parameter value moves past the bifurcation point (Figure 3a).
507 However, when aggregations emerge, they appear suddenly (Figure 3b), with a small change in
508 parameter value causing a sudden jump from homogeneous patterns to clearly-defined aggrega-
509 tions. Moreover, this is accompanied by a hysteresis effect, meaning that identical underlying
510 processes can give rise to either aggregation or homogeneity, depending on the history of the
511 system.

512 As well as using our methods to analyse IBMs, it is conceivable that the same methods
513 may be valuable for analysing pattern formation in empirical data. One would, admittedly,
514 need some rather high quality data: large quantities of co-tagged animals for sufficiently long
515 time periods to observe changes in space use patterns. However, in the present ‘golden age’ of
516 animal movement data (Wilmers *et al.*, 2015), with ongoing rapid increases in the magnitude
517 and quality of datasets (Williams *et al.*, 2020), it is good idea to ensure the methodological
518 and theoretical tools exist to deal with such data as it emerges. We have not focused on data
519 analysis here, but we encourage researchers to test this idea in future studies if they have such
520 data.

521 On the more ecological side, we have shown how accounting for feedbacks between the
522 movement mechanisms of constituent populations may help explain the emergence of intersti-
523 tial regions in territorial animals that could provide safe-havens for weaker competitors. Such
524 patterns have been observed in coexistent wolf and coyote populations in the Greater Yellow-
525 stone Ecosystem. There, these interstitial regions have also been observed as refuges for deer
526 (Lewis & Murray, 1993). Although we did not consider the mobility of prey resources in our

527 simple example, one could add extra complexity by considering the attempts of mobile prey to
528 avoid predators, and observe how this affects the spatial patterns. However, for the purposes
529 of our simple illustration, this level of modelling complexity was not required.

530 An important thing to note is that emergent patterns from interacting populations cannot
531 be revealed by correlative models alone. To take the example from Figure 5, if one knew the
532 distribution of the stronger population, one could perform resource selection analysis with this
533 distribution and the resource layer as the two explanatory variables to understand how these
534 drive space use of the weaker population. However, to use this in a novel environment to predict
535 space use of the weaker population, one would need to know *a priori* the distribution of the
536 stronger. If one wants to predict space use of both populations at the same time, in situations
537 where there is no *a priori* knowledge of either population, resource selection functions are not
538 enough. Instead, one could perform step selection analysis for both interacting population,
539 for example using the techniques of Schlägel *et al.* (2019), then feed the output of this into
540 a movement kernel in the form of Equation (1), for example using the techniques of Potts
541 & Schlägel (2020). This would lead to precisely the sort of IBM studied here, which enables
542 analysis of predicted space use patterns in novel environments.

543 In general, our approach is valuable for predicting the distribution of populations whenever
544 the locations of two or more populations affect the movements of each other (Schlägel *et al.*,
545 2020). This has been observed in a variety of situations. We have already mentioned com-
546 petition between carnivores, and indeed the movements of coexistent carnivore populations in
547 response to the presence of others has been measured in various studies (Vanak *et al.*, 2013;
548 Swanson *et al.*, 2016). Also the effect of predator movement on prey locations (sometimes
549 called prey-taxis), and vice versa (the ‘landscape of fear’), has been documented in a variety of
550 scenarios (Kareiva & Odell, 1987; Laundré *et al.*, 2010; Latombe *et al.*, 2014; Gallagher *et al.*,
551 2017). Despite this, the predominant species distributions models used in ecology tend to
552 not to account for the underlying between-population movement processes and the emergent
553 features that they engender, even in cases where they model species jointly (Ovaskainen &

554 Abrego, 2020). Explicit modelling of the underlying movement mechanisms, as we have done
555 here, would help plug this gap and lead to more accurate description and forecasting of species
556 distributions.

557 **Acknowledgements**

558 JRP and VG acknowledge support of Engineering and Physical Sciences Research Council
559 (EPSRC) grant EP/V002988/1. MAL acknowledges support from the NSERC Discovery
560 and Canada Research Chair programs. The authors thank Jason Matthiopoulos, together
561 with anonymous reviewers and editors, for comments that have helped greatly improve the
562 manuscript.

563 **Author contributions**

564 JRP and MAL conceived and designed the research. JRP and VG performed the research.
565 JRP led the writing of the manuscript. All authors contributed critically to the drafts and
566 gave final approval for publication.

567 **References**

568 1.

569 Arjo, W.M. & Pletscher, D.H. (2000). Behavioral responses of coyotes to wolf recolonization
570 in northwestern montana. *Can. J Zool.*, 77, 1919–1927.

571 2.

572 Avgar, T., Potts, J.R., Lewis, M.A. & Boyce, M.S. (2016). Integrated step selection analysis:
573 bridging the gap between resource selection and animal movement. *Methods Ecol. Evol.*, 7,
574 619–630.

575 3.

576 Azaele, S., Maritan, A., Cornell, S.J., Suweis, S., Banavar, J.R., Gabriel, D. & Kunin, W.E.
577 (2015). Towards a unified descriptive theory for spatial ecology: predicting biodiversity
578 patterns across spatial scales. *Methods Ecol. Evol.*, 6, 324–332.

579 4.

580 Bastille-Rousseau, G., Potts, J.R., Schaefer, J.A., Lewis, M.A., Ellington, E.H., Rayl, N.D.,
581 Mahoney, S.P. & Murray, D.L. (2015). Unveiling trade-offs in resource selection of migratory
582 caribou using a mechanistic movement model of availability. *Ecography*, 38, 1049–1059.

583 5.

584 Berens, P. (2009). Circstat: a matlab toolbox for circular statistics. *J Stat. Softw.*, 31, 1–21.

585 6.

586 Breed, G.A., Matthews, C.J., Marcoux, M., Higdon, J.W., LeBlanc, B., Petersen, S.D., Orr,
587 J., Reinhart, N.R. & Ferguson, S.H. (2017). Sustained disruption of narwhal habitat use and
588 behavior in the presence of arctic killer whales. *Proc. Nat. Acad. Sci.*, 114, 2628–2633.

589 7.

590 Buttenschön, A. & Buttenschön (2021). *Non-Local Cell Adhesion Models*. Springer.

591 8.

592 Cantrell, R.S. & Cosner, C. (2004). *Spatial ecology via reaction-diffusion equations*. John
593 Wiley & Sons, Chichester.

594 9.

595 Codling, E.A., Plank, M.J. & Benhamou, S. (2008). Random walk models in biology. *J.*
596 *Roy. Soc. Interface*, 5, 813–834.

597 10.

598 DeAngelis, D.L. (2018). *Individual-based models and approaches in ecology: populations,*
599 *communities and ecosystems*. CRC Press.

600 11.

601 Durrett, R. & Levin, S. (1994). The importance of being discrete (and spatial). *Theor. Pop.*
602 *Biol.*, 46, 363–394.

603 12.

604 Eftimie, R., de Vries, G. & Lewis, M. (2009). Weakly nonlinear analysis of a hyperbolic
605 model for animal group formation. *J. Math. Biol.*, 59, 37–74.

606 13.

607 Ellison, N., Hatchwell, B.J., Biddiscombe, S.J., J, N.C. & Potts, J.R. (2020). Mechanistic
608 home range analysis reveals drivers of space use patterns for a non-territorial passerine. *J*
609 *Anim. Ecol.*, 89, 2763–76.

610 14.

611 Elton, C.S. (2001). *Animal ecology*. University of Chicago Press.

612 15.

613 Evans, L.C. (2010). *Partial differential equations*. American Mathematical Society, Provi-
614 dence, Rhode Island.

615 16.

616 Fieberg, J. & Kochanny, C.O. (2005). Quantifying home-range overlap: The importance of
617 the utilization distribution. *J Wildlife Manage.*, 69, 1346–1359.

618 17.

619 Fleming, C.H., Fagan, W.F., Mueller, T., Olson, K.A., Leimgruber, P. & Calabrese, J.M.
620 (2015). Rigorous home range estimation with movement data: a new autocorrelated kernel
621 density estimator. *Ecology*, 96, 1182–1188.

622 18.

623 Fortin, D., Beyer, H., Boyce, M., Smith, D., Duchesne, T. & Mao, J. (2005). Wolves influence

624 elk movements: Behavior shapes a trophic cascade in yellowstone national park. *Ecology*,
625 86, 1320–1330.

626 19.

627 Gallagher, A.J., Creel, S., Wilson, R.P. & Cooke, S.J. (2017). Energy landscapes and the
628 landscape of fear. *Trends Ecol. Evol.*, 32, 88–96.

629 20.

630 Gambino, G., Lombardo, M.C. & Sammartino, M. (2013). Pattern formation driven by
631 cross-diffusion in a 2d domain. *Nonlinear Analysis: Real World Applications*, 14, 1755–1779.

632 21.

633 Getz, W.M., Marshall, C.R., Carlson, C.J., Giuggioli, L., Ryan, S.J., Romañach, S.S., Boet-
634 tiger, C., Chamberlain, S.D., Larsen, L., D’Odorico, P. *et al.* (2018). Making ecological
635 models adequate. *Ecol. Lett.*, 21, 153–166.

636 22.

637 Giuggioli, L., Potts, J.R. & Harris, S. (2011). Animal interactions and the emergence of
638 territoriality. *PLoS Comput. Biol.*, 7, e1002008.

639 23.

640 Giuggioli, L., Potts, J.R., Rubenstein, D.I. & Levin, S.A. (2013). Stigmergy, collective
641 actions, and animal social spacing. *Proc. Nat. Acad. Sci.*, p. 201307071.

642 24.

643 Grimm, V. (1999). Ten years of individual-based modelling in ecology: what have we learned
644 and what could we learn in the future? *Ecol. Model.*, 115, 129–148.

645 25.

646 Grimm, V. & Railsback, S.F. (2013). *Individual-based modeling and ecology*. Princeton
647 university press.

648 26.

649 Han, R. & Dai, B. (2019). Spatiotemporal pattern formation and selection induced by nonlin-
650 ear cross-diffusion in a toxic-phytoplankton–zooplankton model with allee effect. *Nonlinear*
651 *Analysis: Real World Applications*, 45, 822–853.

652 27.

653 Haskell, E.C. & Bell, J. (2020). Pattern formation in a predator-mediated coexistence model
654 with prey-taxis. *Discrete & Continuous Dynamical Systems-B*, 25, 2895.

655 28.

656 Hillen, T. & Painter, K. (2013). Transport and anisotropic diffusion models for movement in
657 oriented habitats. In: *Dispersal, Individual Movement and Spatial Ecology* (eds. Lewis, M.A.,
658 Maini, P.K. & Petrovskii, S.V.). Springer Berlin Heidelberg, Lecture Notes in Mathematics,
659 pp. 177–222.

660 29.

661 Holmes, E.E., Lewis, M.A., Banks, J. & Veit, R. (1994). Partial differential equations in
662 ecology: spatial interactions and population dynamics. *Ecology*, 75, 17–29.

663 30.

664 Hosseini, P.R. (2006). Pattern formation and individual-based models: the importance of
665 understanding individual-based movement. *Ecol. Model.*, 194, 357–371.

666 31.

667 Kareiva, P. & Odell, G. (1987). Swarms of predators exhibit "prey taxis" if individual
668 predators use area-restricted search. *Am. Nat.*, 130, 233–270.

669 32.

670 Latombe, G., Fortin, D. & Parrott, L. (2014). Spatio-temporal dynamics in the response of
671 woodland caribou and moose to the passage of grey wolf. *J Anim. Ecol.*, 83, 185–198.

672 33.

673 Laundré, J.W., Hernández, L. & Ripple, W.J. (2010). The landscape of fear: ecological
674 implications of being afraid. *Open Ecology Journal*, 3, 1–7.

675 34.

676 Lee, J., Hillen, T. & Lewis, M. (2009). Pattern formation in prey-taxis systems. *J. Biol.*
677 *Dynam.*, 3, 551–573.

678 35.

679 Lewis, M.A., Maini, P.K. & Petrovskii, S.V. (2013). Dispersal, individual movement and
680 spatial ecology. *Lecture Notes in Mathematics (Mathematics Bioscience Series)*, 2071.

681 36.

682 Lewis, M.A. & Murray, J.D. (1993). Modelling territoriality and wolf-deer interactions.
683 *Nature*, 366, 738–740.

684 37.

685 Lewis, M.A., Petrovskii, S.V. & Potts, J.R. (2016). *The mathematics behind biological inva-*
686 *sions*. Springer, Switzerland.

687 38.

688 Maris, V., Huneman, P., Coreau, A., Kéfi, S., Pradel, R. & Devictor, V. (2018). Prediction
689 in ecology: promises, obstacles and clarifications. *Oikos*, 127, 171–183.

690 39.

691 Matthews, C.J., Breed, G.A., LeBlanc, B. & Ferguson, S.H. (2020). Killer whale presence
692 drives bowhead whale selection for sea ice in arctic seascapes of fear. *Proc. Nat. Acad. Sci.*,
693 117, 6590–6598.

694 40.

695 May, R.M. (2019). *Stability and complexity in model ecosystems*. Princeton University Press.

696 41.

697 Mitchell, W.A. & Lima, S.L. (2002). Predator-prey shell games: large-scale movement and
698 its implications for decision-making by prey. *Oikos*, 99, 249–259.

699 42.

700 Moorcroft, P.R., Lewis, M.A. & Crabtree, R.L. (2006). Mechanistic home range models
701 capture spatial patterns and dynamics of coyote territories in yellowstone. *Proc. Roy. Soc.*
702 *B*, 273, 1651–1659.

703 43.

704 Morales, J.M., Moorcroft, P.R., Matthiopoulos, J., Frair, J.L., Kie, J.G., Powell, R.A.,
705 Merrill, E.H. & Haydon, D.T. (2010). Building the bridge between animal movement and
706 population dynamics. *Phil. T. R. Soc. B*, 365, 2289–2301.

707 44.

708 Murray, J.D. (2012). *Asymptotic analysis*. vol. 48. Springer Science & Business Media.

709 45.

710 Nathan, R., Getz, W.M., Revilla, E., Holyoak, M., Kadmon, R., Saltz, D. & Smouse, P.E.
711 (2008). A movement ecology paradigm for unifying organismal movement research. *Proc.*
712 *Nat. Acad. Sci.*, 105, 19052–19059.

713 46.

714 Okubo, A. & Levin, S.A. (2001). *Diffusion and ecological problems: modern perspectives*.
715 vol. 14. Springer.

716 47.

717 Ovaskainen, O. & Abrego, N. (2020). *Joint species distribution modelling: with applications*
718 *in R*. Cambridge University Press.

719 48.

720 Painter, K.J. & Hillen, T. (2011). Spatio-temporal chaos in a chemotaxis model. *Physica D*,
721 240, 363–375.

722 49.

723 Potts, J., Bastille-Rousseau, G., Murray, D., Schaefer, J. & Lewis, M. (2014a). Predicting
724 local and non-local effects of resources on animal space use using a mechanistic step-selection
725 model. *Methods Ecol. Evol.*, 5, 253–262.

726 50.

727 Potts, J.R., Auger-Méthé, M., Mokross, K. & Lewis, M.A. (2014b). A generalized residual
728 technique for analysing complex movement models using earth mover’s distance. *Methods*
729 *Ecol. Evol.*, 5, 1012–1022.

730 51.

731 Potts, J.R., Harris, S. & Giuggioli, L. (2012). Territorial dynamics and stable home range
732 formation for central place foragers. *PLoS One*, 7, e34033.

733 52.

734 Potts, J.R. & Lewis, M.A. (2016). Territorial pattern formation in the absence of an attractive
735 potential. *J Math. Biol.*, 72, 25–46.

736 53.

737 Potts, J.R. & Lewis, M.A. (2019). Spatial memory and taxis-driven pattern formation in
738 model ecosystems. *Bull. Math. Biol.*, 81, 2725–2747.

739 54.

740 Potts, J.R., Mokross, K. & Lewis, M.A. (2014c). A unifying framework for quantifying the
741 nature of animal interactions. *J Roy. Soc. Interface*, 11, 20140333.

742 55.

743 Potts, J.R. & Painter, K.J. (2021). Stable steady-state solutions of some biological aggrega-
744 tion models. *SIAM J Appl. Math.*, 81, 1248–1263.

745 56.

746 Potts, J.R. & Petrovskii, S.V. (2017). Fortune favours the brave: Movement responses shape
747 demographic dynamics in strongly competing populations. *J. Theor. Biol.*, 420, 190–199.

748 57.

749 Potts, J.R. & Schlägel, U.E. (2020). Parametrizing diffusion-taxis equations from animal
750 movement trajectories using step selection analysis. *Methods Ecol. Evol.*, 11, 1092–105.

751 58.

752 Schlägel, U.E., Grimm, V., Blaum, N., Colangeli, P., Dammhahn, M., Eccard, J.A., Haus-
753 mann, S.L., Herde, A., Hofer, H., Joshi, J. *et al.* (2020). Movement-mediated community
754 assembly and coexistence. *Biol. Rev.*, 95, 1073–1096.

755 59.

756 Schlägel, U.E., Signer, J., Herde, A., Eden, S., Jeltsch, F., Eccard, J.A. & Dammhahn,
757 M. (2019). Estimating interactions between individuals from concurrent animal movements.
758 *Methods Ecol. Evol.*

759 60.

760 Sherratt, J.A., Eagan, B.T. & Lewis, M.A. (1997). Oscillations and chaos behind predator–
761 prey invasion: mathematical artifact or ecological reality? *Phil. T. R. Soc. B*, 352, 21–38.

762 61.

763 Shigesada, N., Kawasaki, K. & Teramoto, E. (1979). Spatial segregation of interacting
764 species. *J Theor. Biol.*, 79, 83–99.

765 62.

766 Signer, J., Fieberg, J. & Avgar, T. (2017). Estimating utilization distributions from fitted
767 step-selection functions. *Ecosphere*, 8, e01771.

768 63.

769 Swanson, A., Arnold, T., Kosmala, M., Forester, J. & Packer, C. (2016). In the absence of
770 a “landscape of fear”: How lions, hyenas, and cheetahs coexist. *Ecol. Evol.*, 6, 8534–8545.

771 64.

772 Theraulaz, G. & Bonabeau, E. (1999). A brief history of stigmergy. *Artif. Life*, 5, 97–116.

773 65.

774 Tilman, D., Kareiva, P.M. *et al.* (1997). *Spatial ecology: the role of space in population*
775 *dynamics and interspecific interactions*. Princeton University Press.

776 66.

777 Turing, A.M. (1952). The chemical basis of morphogenesis. *Phil. Trans. R. Soc. Lond. B*,
778 237, 37–72.

779 67.

780 Vanak, A., Fortin, D., Thakera, M., Ogdene, M., Owena, C., Greatwood, S. & Slotow, R.
781 (2013). Moving to stay in place - behavioral mechanisms for coexistence of african large
782 carnivores. *Ecology*, 94, 2619–2631.

783 68.

784 White, L.A., VandeWoude, S. & Craft, M.E. (2020). A mechanistic, stigmergy model of
785 territory formation in solitary animals: Territorial behavior can dampen disease prevalence
786 but increase persistence. *PLoS Comput. Biol.*, 16, e1007457.

787 69.

788 Williams, H.J., Taylor, L.A., Benhamou, S., Bijleveld, A.I., Clay, T.A., de Grissac, S.,
789 Demšar, U., English, H.M., Franconi, N., Gómez-Laich, A. *et al.* (2020). Optimizing the use
790 of biologgers for movement ecology research. *J Anim. Ecol.*, 89, 186–206.

791 70.

792 Wilmers, C.C., Nickel, B., Bryce, C.M., Smith, J.A., Wheat, R.E. & Yovovich, V. (2015).

793 The golden age of bio-logging: how animal-borne sensors are advancing the frontiers of
794 ecology. *Ecology*, 96, 1741–1753.

795 71.

796 Worton, B.J. (1989). Kernel methods for estimating the utilization distribution in home-
797 range studies. *Ecology*, 70, 164–168.